Molecular Therapy
Oncology
Original Article

Bispecific CAR-T cells targeting FAP and GPC3 have the potential to treat hepatocellular carcinoma

Linfu Zhou,[1,2,7] Yao Li,[1,2,7] Diwei Zheng,[1] Yongfang Zheng,[1,2] Yuanbin Cui,[1] Le Qin,[1,3,4] Zhaoyang Tang,[4] Dongdong Peng,[1,2] Qiting Wu,[1] Youguo Long,[1] Yao Yao,[1] Nathalie Wong,[5] James Lau,[5] and Peng Li[1,2,3,5,6]

[1]China-New Zealand Joint Laboratory of Biomedicine and Health, State Key Laboratory of Respiratory Disease, Guangdong Provincial Key Laboratory of Stem Cell and Regenerative Medicine, the CUHK-GIBH Joint Research Laboratory on Stem Cell and Regenerative Medicine, Guangzhou Institutes of Biomedicine and Health, Chinese Academy of Sciences, Guangzhou, China; [2]University of Chinese Academy of Sciences, Beijing 100049, China; [3]Centre for Regenerative Medicine and Health, Hong Kong Institute of Science & Innovation, Chinese Academy of Sciences, Hong Kong SAR, China; [4]Guangdong Zhaotai Cell Biology Technology Ltd., Foshan, China; [5]Department of Surgery of the Faculty of Medicine, the Chinese University of Hong Kong (CUHK), Hong Kong, China; [6]Key Laboratory of Biological Targeting Diagnosis, Therapy and Rehabilitation of Guangdong Higher Education Institutes, The Fifth Affiliated Hospital of Guangzhou Medical University, Guangzhou, China

Chimeric antigen receptor (CAR) T cell therapy has demonstrated robust efficacy against hematological malignancies, but there are still some challenges regarding treating solid tumors, including tumor heterogeneity, antigen escape, and an immunosuppressive microenvironment. Here, we found that SNU398, a hepatocellular carcinoma (HCC) cell line, exhibited high expression levels of fibroblast activation protein (FAP) and Glypican 3 (GPC3), which were negatively correlated with patient prognosis. The HepG2 HCC cell line highly expressed GPC3, while the SNU387 cell line exhibited high expression of FAP. Thus, we developed bispecific CAR-T cells to simultaneously target FAP and GPC3 to address tumor heterogeneity in HCC. The anti-FAP-GPC3 bispecific CAR-T cells could recognize and be activated by FAP or GPC3 expressed by tumor cells. Compared with anti-FAP CAR-T cells or anti-GPC3 CAR-T cells, bispecific CAR-T cells achieved more robust activity against tumor cells expressing FAP and GPC3 *in vitro*. The anti-FAP-GPC3 bispecific CAR-T cells also exhibited superior antitumor efficacy and significantly prolonged the survival of mice compared with single-target CAR-T cells *in vivo*. Overall, the use of anti-FAP-GPC3 bispecific CAR-T cells is a promising treatment approach to reduce tumor recurrence caused by tumor antigen heterogeneity.

INTRODUCTION

Liver cancer continues to be a significant global health issue that poses a threat to human health.[1,2] It is estimated that the number of people affected by liver cancer will exceed 1 million by 2025.[3] The most common histological type of liver cancer is hepatocellular carcinoma (HCC) (75%–80%).[4] In addition to conventional surgical treatment, therapies such as CAR-T cell therapy, immune checkpoint inhibitors (ICIs), tyrosine kinase inhibitors (TKIs), and antibody treatment have the potential to extend patient survival.[5] However, despite the availability of these therapeutic options, HCC remains an incurable disease due to tumor heterogeneity.[6]

Adoptive transfer of CAR-T cells is an effective strategy to suppress tumor growth and prolong the survival of patients. CAR-T cells are composed of a single-chain variable fragment (scFv) for extracellular antigen binding, a CD3 intracellular signaling domain, and other intracellular costimulatory signaling domains, including CD28 and 4-1BB.[7] The success of anti-CD19 CAR-T cells has benefited patients with hematological malignancies[7,8] and has inspired the development of CAR-T cells targeting various antigens. However, CAR-T cell therapy still faces several challenges in the treatment of solid tumors, including a lack of potent therapeutic targets, tumor heterogeneity, the suppressive tumor microenvironment, and antigen escape.[9] To address these issues, it is essential to identify additional tumor-associated biomarkers to reduce antigen escape and maximize the therapeutic efficacy of CAR-T cells.

Glypican 3 (GPC3) is a highly tumor-associated antigen that is expressed during fetal development but is strictly suppressed in the normal adult liver.[10,11] However, in HCC, more than 70% of cases express high levels of GPC3[12,13], and nearly 90% of liver cancers express high levels of GPC3.[1] Previous studies have recognized the potential for using GPC3-targeting antibodies or CAR-T cells to treat liver cancer.[10,14–18] Specifically, some phase I clinical trials of GPC3 CAR-T cells for the treatment of patients with HCC and liver cancer have been initiated.[15,18,19] Although GPC3 CAR-T cells have shown some clinical efficacy,[20] they still face certain challenges when used

Received 15 September 2023; accepted 21 May 2024;
https://doi.org/10.1016/j.omton.2024.200817.

[7]These authors contributed equally

Correspondence: Peng Li, China-New Zealand Joint Laboratory of Biomedicine and Health, State Key Laboratory of Respiratory Disease, Guangdong Provincial Key Laboratory of Stem Cell and Regenerative Medicine, the CUHK-GIBH Joint Research Laboratory on Stem Cell and Regenerative Medicine, Guangzhou Institutes of Biomedicine and Health, Chinese Academy of Sciences, Guangzhou, China.
E-mail: li_peng@gibh.ac.cn

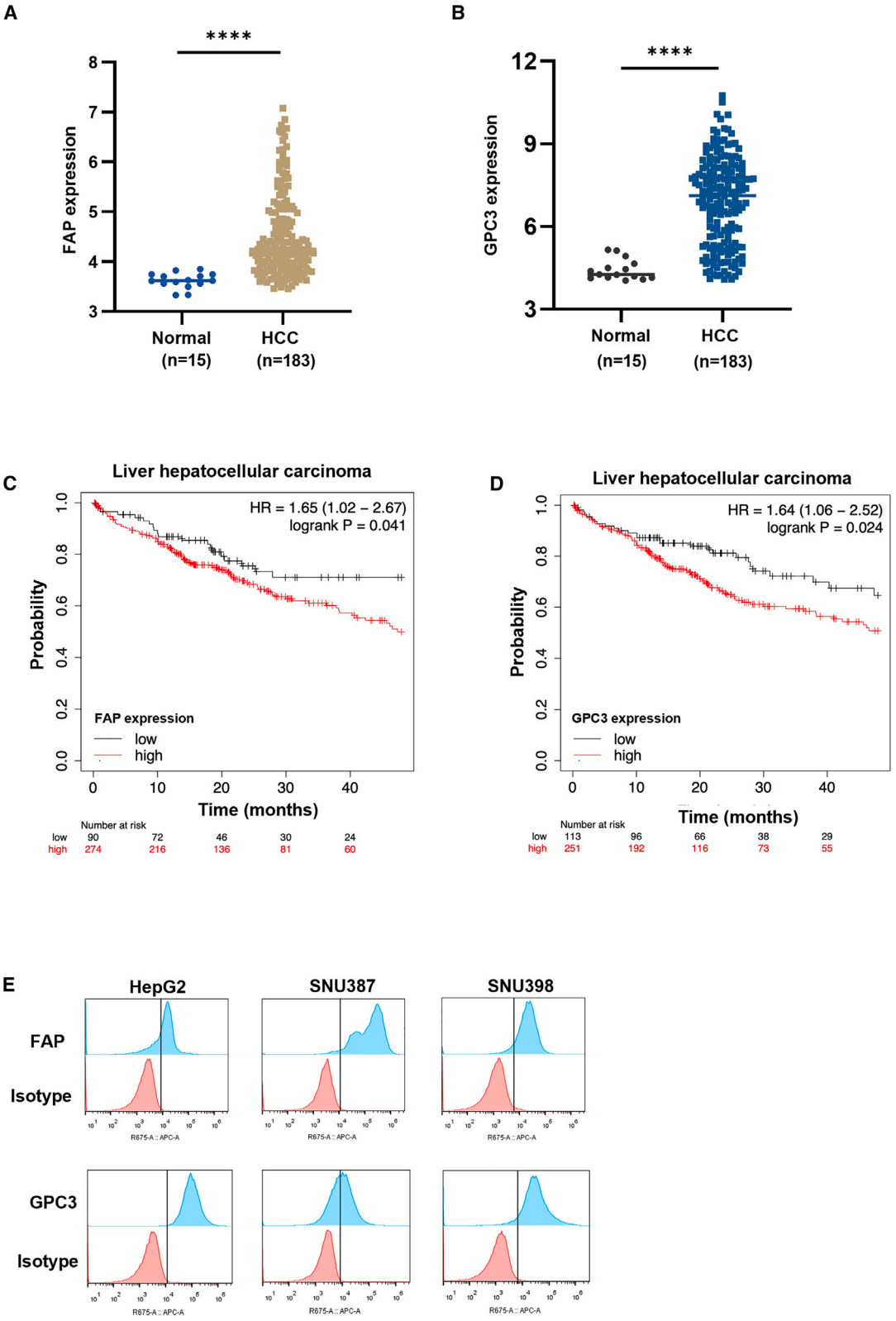

(legend on next page)

to treat liver cancers, including tumor heterogeneity and antigen escape. It has been reported that GPC3 would shed and GPC3 shedding would lead to poor response of anti-GPC3 CAR-T cells in the treatment of HCC.[21] Therefore, it is necessary to develop a CAR-T cell therapy that avoids antigen escape due to GPC3 shedding in HCC.

Fibroblast activation protein (FAP) is a type-II transmembrane serine protease secreted by fibroblasts.[22] In normal tissues, FAP remodels the extracellular matrix to allow for tissue remodeling.[23] Anti-FAP CAR-T cells have been used to treat cardiac injury.[24] In liver carcinogenesis, FAP promotes fibrosis during early liver injury, tumor cell proliferation, and immune suppression.[25] Additionally, FAP is secreted by cancer-associated fibroblasts (CAFs) and plays an important role in remodeling the tumor microenvironment and promoting tumor progression in various cancers.[25–28] FAP expression also correlates with poor clinical outcomes.[29] Consequently, FAP plays a major role in promoting the development of HCC. Targeting FAP in HCC may enhance the antitumor effects of CAR-T cells.

We presented a novel design of CAR-T cells constructed with two scFvs that simultaneously target GPC3 and FAP to expand CAR-T cell therapy to additional indications and tumor antigens. The bispecific CAR-T cells could recognize and kill HCC cells *in vitro* by simultaneously targeting GPC3 and FAP, indicating that both GPC3 scFv and FAP scFv are capable of interacting with tumor antigens and transmitting signals downstream. Moreover, the bispecific CAR-T cells demonstrated significant increases in the efficacy against HCC with high expression of GPC3 or FAP relative to GPC3 CAR-T and FAP CAR-T cells. *In vivo* studies revealed that these bispecific CAR-T cells suppressed HCC tumor growth and prolonged the survival of tumor-bearing mice, providing evidence of their ability to prevent antigen evasion and control heterogeneous HCC.

RESULTS

FAP and GPC3 are highly expressed in HCC

First, we sought to investigate the feasibility of using FAP and GPC3 as viable targets for CAR-T cell therapy to treat HCC. Data from the Cancer Dependency Map suggested that both FAP and GPC3 were broadly expressed in various types of HCC cell lines (Figures S1A and S1B) and were significantly elevated in primary HCC samples based on the GEO database (Figures 1A and 1B). Moreover, the high expression of FAP and GPC3 was associated with poor prognoses for HCC patients (Figures 1C and 1D). In addition, our previous study showed that FAP was highly expressed in induced HCC.[30] We next confirmed the expression of FAP and GPC3 in several HCC cell lines, and the results showed that FAP and GPC3 were highly expressed in HepG2, SNU387, and SNU389 cells (Figure 1E). Taken together, these findings indicated that both FAP and GPC3 could serve as treatment targets for HCC.

Generation and characterization of anti-FAP-GPC3 bispecific CAR-T cells

Given the high expression levels of FAP and GPC3 in HCC and their impact on patient survival, we hypothesized that bispecific anti-FAP and anti-GPC3 CAR-T cells might have enhanced antitumor efficacy for HCC. To verify our hypothesis, we designed a tandem bispecific CAR vector (anti-FAP-GPC3 bispecific CAR) using a humanized single-chain variable fragment (scFv) derived from an anti-human FAP antibody and an anti-human GPC3 antibody that were connected in tandem by a G4S linker (FAP-GPC3 CAR). The FAP-GPC3 CAR construct also included a CD28 costimulatory domain,[31] a CD3ζ intracellular domain and Toll-like receptor 2 (TLR2)[32] and EGFP tag (Figure 2A). CARs targeting human FAP (FAP CAR) and human GPC3 (GPC3 CAR) were constructed as positive controls (Figure 2A). Titers were determined after lentivirus production (Figure S1C). T cells transfected with EGFP (MOCK-T) served as a negative control. CAR expression was indicated by EGFP and was detected by flow cytometry after lentivirus transduction. The lentivirus was efficiently transduced into T cells (Figure S1D) and the CARs were expressed on the surface of T cells (Figure 2B). The proliferation of the CAR-T cells was similar to that of the MOCK-T cells (Figure 2C). It has been reported that T cell activation can be monitored based on changes in the expression of CD25 and CD69.[33] To investigate the independent activation of FAP-GPC3 CAR-T cells by FAP and GPC3 scFvs, we cocultured FAP-GPC3 CAR-T cells with HepG2 cells (low expression of FAP, high expression of GPC3), SNU387 cells (high expression of FAP, low expression of GPC3), and SNU398 cells (high expression of both FAP and GPC3) (Figure 1E). The results showed that FAP-GPC3 CAR-T cells could be activated by HepG2, SNU387, or SNU398 cells (Figures 2D and S1E). Furthermore, to ensure that the two linked scFvs could recognize both FAP and GPC3, we determined the activation efficiency of FAP-GPC3 CAR-T cells by coculturing CAR-T cells with SNU398 cells. Following coculture with SNU398, the expression levels of CD25 and CD69 on CAR-T cells were assessed by flow cytometry. The results demonstrated that single-target CAR-T cells, FAP CAR-T cells and GPC3 CAR-T cells upregulated the expression of CD25 and CD69. Notably, CAR-T cells targeting both FAP and GPC3 exhibited the highest levels of CD25 and CD69 expression (Figures 2E and 2F). These results demonstrated that FAP-GPC3 CAR-T cells could recognize FAP and/or GPC3, thereby activating their function.

FAP-GPC3 CAR-T cells exhibited potent cytotoxicity against HCC cells *in vitro*

The antitumor capacity of FAP-GPC3 CAR-T cells was subsequently evaluated *in vitro*. To assess the cytotoxicity of CAR-T cells efficiently

Figure 1. FAP and GPC3 are highly expressed in HCC

(A) FAP expression in HCC patient tumor tissue. The data were downloaded from the GEO database and analyzed with the Assistant of Clinical Bioinformatics. (B) GPC3 expression in HCC patient tumor tissue. The data were downloaded from the GEO database and analyzed with the Assistant of Clinical Bioinformatics. (C) Analysis of the effect of FAP expression on the prognosis of HCC patients. Data from Kaplan-Meier Plotter. (D) Analysis of the effect of GPC3 expression on the prognosis of HCC patients. Data from Kaplan-Meier Plotter. (E) FAP and GPC3 expression in HepG2, SNU387, and SNU398 cells was detected by flow cytometry.

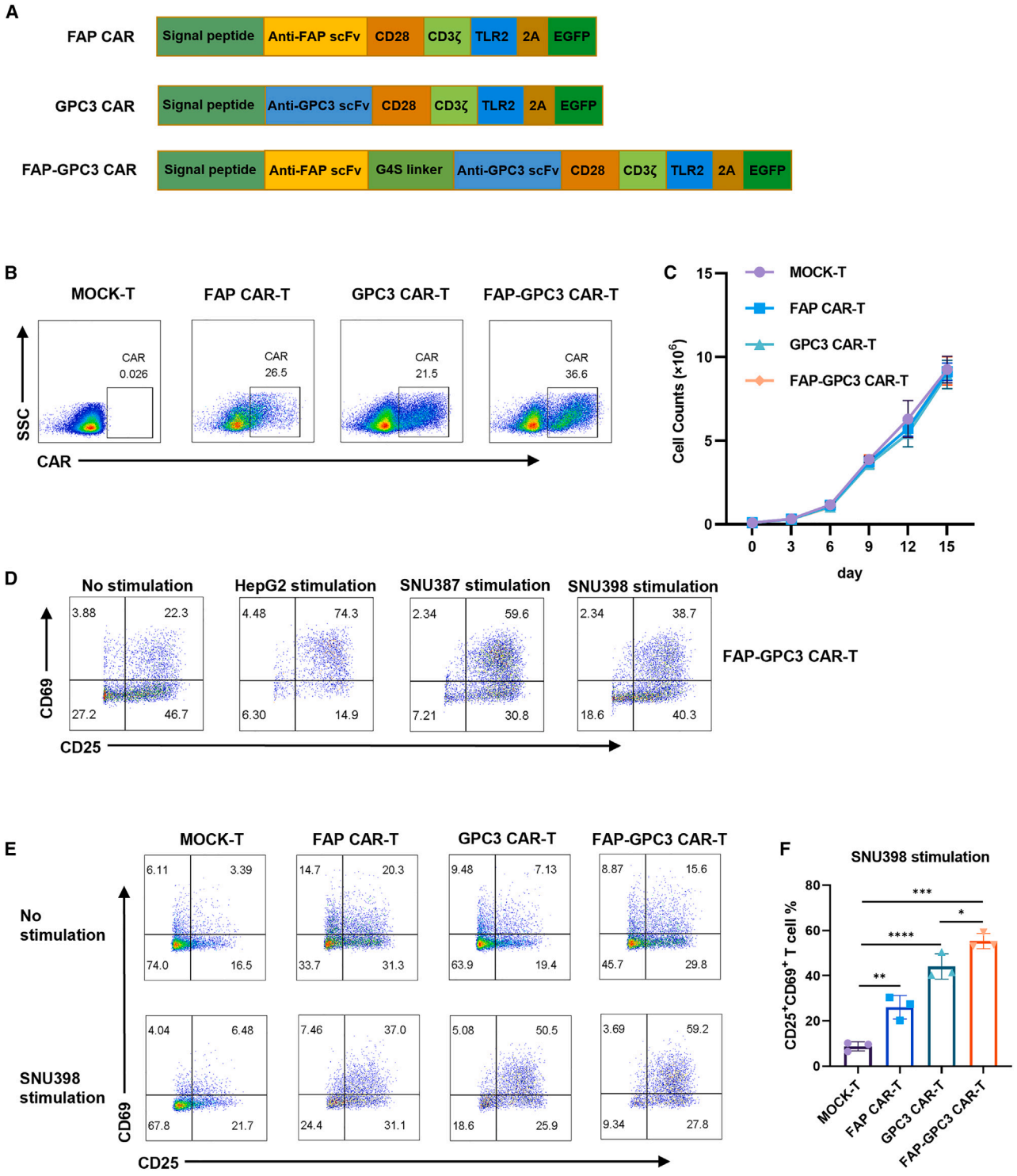

Figure 2. Generation and characterization of anti-FAP-GPC3 bispecific CAR-T cells

(A) Schematic diagrams of FAP CAR, GPC3 CAR, and FAP-GPC3 CAR. (B) The expression of CAR in CAR-T cells was analyzed representatively by flow cytometry. (C) The proliferation of CAR-T cells after transfection. (D) CD25 and CD69 expression on FAP-GPC3 CAR-T cells stimulated with different tumor cells was detected by flow cytometry. (E) CD25 and CD69 expression on CAR-T cells after being cocultured with SNU398 cells was detected by flow cytometry. (F) The statistical results of (E). The data are shown as the mean ± SD; one-way ANOVA with multiple comparisons test; $^{*}p < 0.05$; $^{**}p < 0.01$; $^{***}p < 0.001$; $^{****}p \leq 0.0001$.

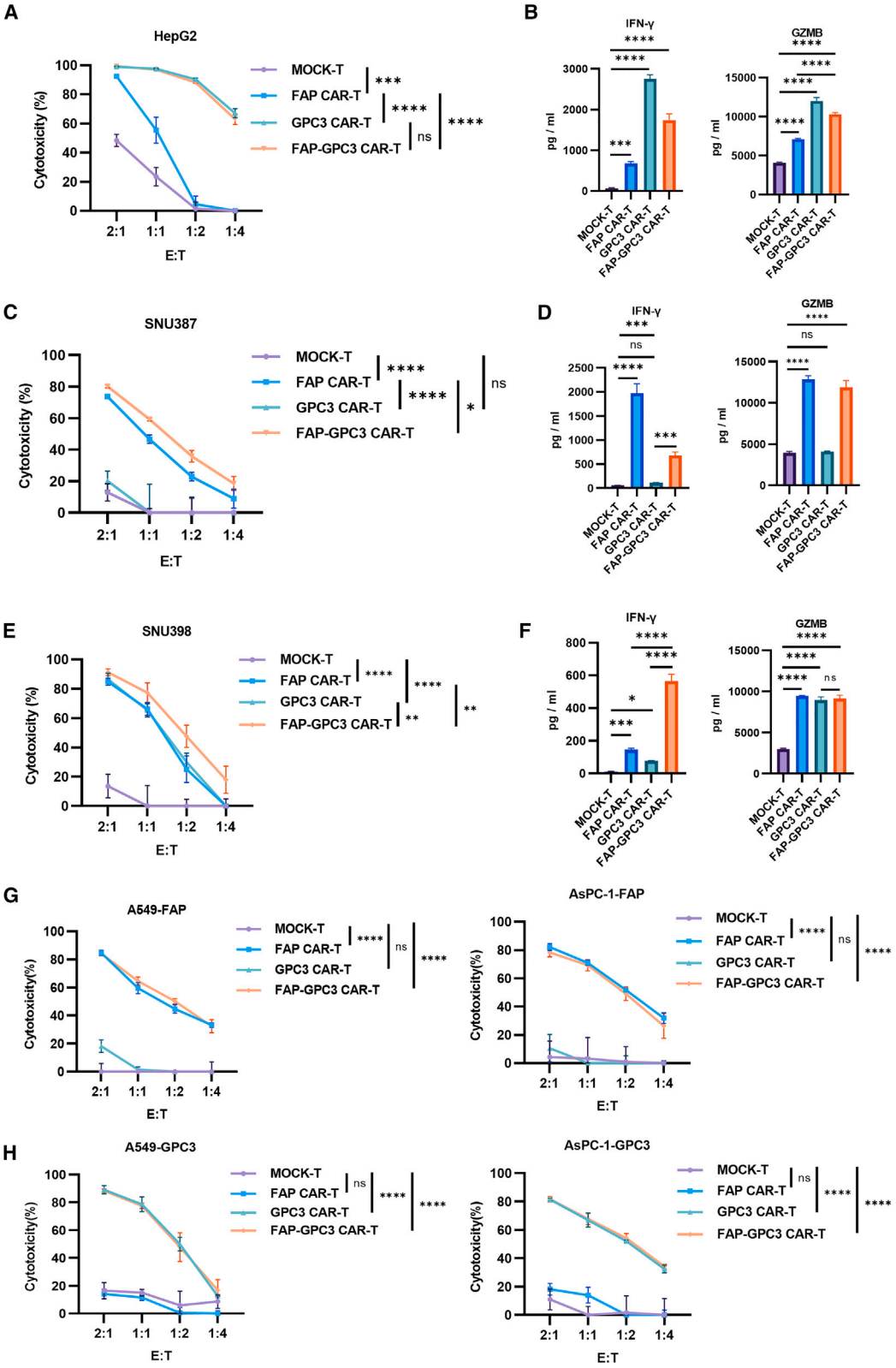

(legend on next page)

and accurately, three HCC cell lines (HepG2, SNU387, and SNU398) were genetically modified to express GFP-luciferase. This genetic modification allowed cell viability to be determined using a luciferase reporter system and an illuminator.[34] CAR-T cells and MOCK-T cells were then incubated with tumor cells at a specified effector T cell:tumor cell (E:T) ratio. The ability of the two scFvs of FAP-GPC3 CAR-T cells to recognize antigens and activate the cytotoxicity of CAR-T cells was determined by incubating FAP-GPC3 CAR-T cells with HepG2, SNU387, and SNU398 cells. FAP-GPC3 CAR-T cells exhibited cytotoxicity against HepG2 cells similar to that of GPC3 CAR-T cells, while the cytotoxicity of FAP CAR-T cells against HepG2 cells was significantly weaker than that of FAP-GPC3 CAR-T cells and GPC3 CAR-T cells but stronger than that of MOCK-T cells (Figure 3A). The results of the killing assay demonstrated that FAP-GPC3 CAR-T cells exhibited similar killing activity as GPC3 CAR-T cells against HCC cells, which express high levels of GPC3 and low levels of FAP. The cytokine secretion profile of CAR-T cells in response to target tumor cells was quantified using enzyme-linked immunosorbent assay (ELISA). Cytokines such as interferon-γ (IFN-γ), granzyme B (GZMB), tumor necrosis factor (TNF)-α, and interleukin (IL)-2, which are generally secreted by cytotoxic or activated T cells, were examined. After incubation with HepG2 cells, the secretion of cytokines by FAP-GPC3 CAR-T cells was significantly higher than that of FAP CAR-T cells and MOCK-T cells but lower than that of GPC3 CAR-T cells (Figures 3B and S1A). To further evaluate the function of FAP scFv, CAR-T cells were incubated with SNU387 cells, which express high levels of FAP and low levels of GPC3. The killing assay results showed that FAP-GPC3 CAR-T cells exhibited similar cytotoxicity against SNU387 cells as FAP CAR-T cells, while GPC3 CAR-T cells were unable to kill SNU387 cells (Figure 3C). The secretion of cytokines was consistent with the results of the killing assay (Figures 3D and S1B), further confirming that the FAP scFv of FAP-GPC3 CAR-T cells could recognize FAP and activate CD3ζ signaling. Moreover, to assess the therapeutic effect of FAP-GPC3 CAR-T cells when targeting FAP and GPC3 double-positive tumors, CAR-T cells were cocultured with SNU398 cells, which highly express both FAP and GPC3. The results demonstrated that FAP-GPC3 CAR-T cells exhibited increased cytotoxicity against SNU398 cells (Figure 3E) and secreted increased levels of interferon (IFN)-γ, GZMB, TNF-α, and IL-2 (Figures 3F and S1C). In order to confirm the specific killing ability of FAP-GPC3 CAR-T cells, we cocultured FAP-GPC3 CAR-T cells with A549 and AsPC1 cell lines, which are devoid of FAP and GPC3 expression (Figure S2D), respectively. The results showed that FAP-GPC3 CAR-T cells did not kill A549 and AsPC1 (Figures S2E and S2F). Furthermore, we overexpressed FAP or GPC3 on A549 and AsPC-1 (Figures S2G and S2H). Then A549-FAP/GPC3 or AsPC-1-FAP/GPC3 were cocultured with the CAR-T cells. The results showed that FAP CAR-T cells and FAP-GPC3 CAR-T cells could kill A549-FAP cells and AsPC-1-FAP cells, and GPC3 CAR-T cells and FAP-GPC3 CAR-T cells could kill A549-GPC3 cells and AsPC-1-GPC3 cells (Figures 3G and 3H). Overall, these results indicated that FAP-GPC3 CAR-T cells could specifically recognize and kill FAP-positive, GPC3-positive, and FAP-GPC3 double-positive cancer cells while exhibiting robust cytotoxicity against FAP-GPC3 double-positive cancer cells *in vitro*.

FAP-GPC3 CAR-T cells showed a potent suppressive effect on HCC tumor models derived from different cell lines

Despite the potent antitumor effects of FAP-GPC3 bispecific CAR-T cells *in vivo*, further validation of their antitumor effects, especially on heterogeneous tumors, as necessary. The HCC cell lines HepG2 and SNU398, which express different levels of FAP and GPC3, were used to validate the antitumor effects of FAP-GPC3 CAR-T cells *in vivo*. First, we established an HCC subcutaneous cell line-derived xenograft (CDX) model of HepG2 cells in NSI mice.[35] HepG2 cells, which express low FAP and highly express GPC3, were transplanted into mice. Subsequently, the mice were administered MOCK-T cells, FAP CAR-T cells, GPC3 CAR-T cells, and FAP-GPC3 CAR-T cells when the tumor nodules were palpable (Figure 4A). Tumor volume was measured twice per week. Compared with MOCK-T cells, FAP CAR-T cells, and GPC3 CAR-T cells, FAP-GPC3 CAR-T cells demonstrated superior antitumor efficacy. Furthermore, mice infused with FAP-GPC3 CAR-T cells had significantly slower tumor growth than those treated with GPC3 CAR-T cells or FAP CAR-T cells (Figures 4B and S2A). Additionally, compared with single-target CAR-T cells, FAP-GPC3 CAR-T cells significantly prolonged the survival rate of the mice (Figure 4C). These results suggested that FAP-GPC3 CAR-T cells exhibited superior efficacy in suppressing HepG2 tumor growth *in vivo*. We also determined the percentage of human T cell infiltration in the peripheral blood (PB) (Figure 4D) and the body weight of mice (Figure 4E). The results demonstrated that there was no difference in the *in vivo* expansion of CAR-T cells between MOCK-T cells and did not affect mouse health, indicating that FAP-GPC3 CAR-T cells possess a favorable safety profile. In conclusion, our data showed that compared with GPC3 CAR-T cells, bispecific CAR-T cells exhibited superior suppression of HepG2 cells that expressed increased levels of GPC3 on their cell surface.

Figure 3. FAP-GPC3 CAR-T cells exhibited potent cytotoxicity against HCC cells *in vitro*

Results of killing assays performed with MOCK-T, FAP CAR-T, GPC3 CAR-T, and FAP-GPC3 CAR-T cells targeting HepG2 cells (A), SNU387 cells (C), and SNU398 cells (E). The data are shown as the mean ± SD; two-way ANOVA with Tukey's multiple comparisons test; $^{*}p < 0.05$; $^{**}p < 0.01$; $^{***}p < 0.001$; $^{****}p \leq 0.0001$. The concentrations of IFN-γ and GZMB released by CAR-T cells and MOCK-T cells after being cocultured with HepG2 cells (B), SNU387 (D), and SNU398 (F) for 24 h at an E:T ratio of 1:1. The data are shown as the mean ± SD; unpaired t test. $^{*}p < 0.05$; $^{**}p < 0.01$; $^{***}p < 0.001$; $^{****}p \leq 0.0001$. (G) Results of killing assays performed with MOCK-T, FAP CAR-T, GPC3 CAR-T, and FAP-GPC3 CAR-T cells targeting A549-FAP cells and AsPC-1-FAP cells. The data are shown as the mean ± SD; two-way ANOVA with Tukey's multiple comparisons test; $^{*}p < 0.05$; $^{**}p < 0.01$; $^{***}p < 0.001$; $^{****}p \leq 0.0001$. (H) Results of killing assays performed with MOCK-T, FAP CAR-T, GPC3 CAR-T, and FAP-GPC3 CAR-T cells targeting A549-GPC3 cells and AsPC-1-GPC3 cells. The data are shown as the mean ± SD; two-way ANOVA with Tukey's multiple comparisons test; $^{*}p < 0.05$; $^{**}p < 0.01$; $^{***}p < 0.001$; $^{****}p \leq 0.0001$.

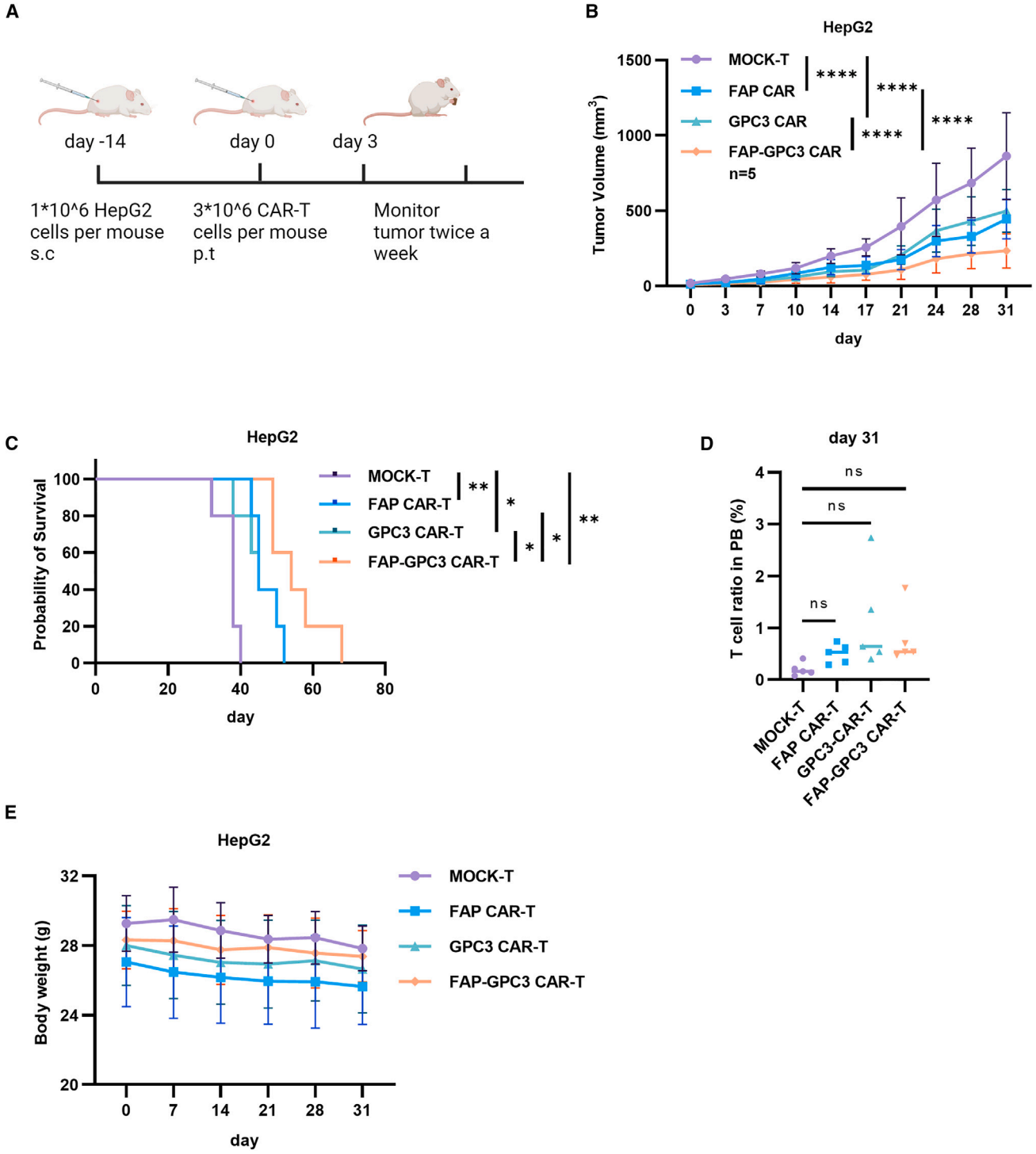

Figure 4. FAP-GPC3 CAR-T cells showed a potent suppressive effect on HepG2 CDX

(A) Schematic representation of the animal experiments with HepG2 CDX model. The graphical abstract was created with BioRender.com, agreement number: ZX25RFJYBS. (B) Measurement of tumor volumes after treatment with CAR-T cells. The data are shown as the mean ± SD; two-way ANOVA with Tukey's multiple comparisons test; *$p < 0.05$; **$p < 0.01$; ***$p < 0.001$; ****$p \leq 0.0001$. (C) Kaplan-Meier survival curve showing overall survival; log rank (Mantel-Cox) test; *$p < 0.05$; **$p < 0.01$. (D) Human T cell ratios in the peripheral blood of HepG2 CDX model mice were detected by flow cytometry. The data are shown as the mean ± SD; two-way ANOVA with Tukey's multiple comparisons test. (E) Mouse body weight in the HepG2 CDX model.

To further investigate the potential interference of the tandem connection between anti-FAP and anti-GPC3 scFv in the antitumor activity of the CAR *in vivo*, we established a mouse model using the SNU398 HCC cell line, which exhibits high expression of both GPC3 and FAP (Figure 5A). Tumor volume was measured every 3 days. Both FAP CAR-T cells and GPC3 CAR-T cells efficiently restricted tumor growth, and FAP-GPC3 CAR-T cells demonstrated significant additional suppression of tumor growth as the tumor volume increased (Figures 5B and S2B). Furthermore, single-target CAR-T cells partially inhibited tumor growth and extended the survival time of mice from 17 to 25 days, whereas FAP-GPC3 CAR-T cells further extended mouse survival from 25 to 41 days (Figure 5C). These results demonstrated that SNU398 tumor growth was further repressed by FAP-GPC3 CAR-T cells in comparison with FAP CAR-T cells and GPC3 CAR-T cells. Additionally, we assessed the percentage of T cell infiltration in the PB, which showed that FAP-GPC3 CAR-T cells were expanded in mice (Figure 5D), and body weight was nearly unchanged (Figure 5E). These results suggested that FAP-GPC3 CAR-T cells exerted potent antitumor effects against tumors expressing FAP or GPC3 *in vivo* and were safe. In conclusion, FAP-GPC3 CAR-T cells effectively suppressed the growth of not only HepG2 tumors but also SNU398 tumors, indicating that FAP-GPC3 CAR-T cells might have a powerful role in combating HCC tumors with heterogeneous antigens.

FAP-GPC3 CAR-T cells exhibited potent activity against HCC patient-derived tumors

FAP-GPC3 CAR-T cells showed stronger cytotoxicity against HCC cell lines *in vitro* and *in vivo*. The widespread heterogeneity of tumors in HCC patients has been reported.[6,36] Here, we used patient-derived xenograft (PDX) of HCC to evaluate the ability of FAP-GPC3 CAR-T cells against a PDX model with tumor heterogeneity. The PDX model was shown to express FAP and GPC3.[30] Patient-derived tissues were transplanted into NSI mice. After 7 days, CAR-T cells were peritumorally injected, and tumor volume was measured every 3 days (Figure 6A). Compared with MOCK-T cells, FAP CAR-T cells, GPC3 CAR-T cells, and FAP-GPC3 CAR-T cells obviously suppressed the growth of PDXs (Figure 6B). FAP-GPC3 CAR-T cells induced stronger suppression than FAP CAR-T cells, and GPC3 CAR-T cells and PDX were eradicated by FAP-GPC3 CAR-T cells (Figures 6B and S2C). Moreover, compared with MOCK-T cells, CAR-T cells markedly prolonged mouse survival (Figure 6C). However, we terminated the animal experiment prematurely on humanitarian grounds due to the significant incidence of graft-vs.-host disease (GVHD) in the majority of mice. FAP-GPC3 CAR-T cells more potently suppressed tumors derived from patients with HCC than FAP CAR-T cells and GPC3 CAR-T cells. In addition, there were no significant differences in the levels of T cells in the PB in the GPC3 CAR-T and FAP-GPC3 CAR-T groups (Figure 6D). Mouse body weight remained unchanged after CAR-T cell infusion (Figure 6E). In brief, FAP-GPC3 CAR-T cells exhibited strong antitumor efficacy in a PDX model that expressed FAP and GPC3 and showed a good safety profile.

DISCUSSION

CAR-T cell therapy achieves striking success in the treatment of patients with hematological malignancies, but no such efficacy has been observed in solid tumors. Antigen recognition is the first step of CAR-T cell killing of tumor cells, and tumor heterogeneity is an obstacle for CAR-T cell therapy, leading to antigen evasion.[37] Solid tumors are heterogeneous, which is different from hematological tumors.[38] In solid tumors, some cells express tumor antigen A, and some express tumor antigen B. However, recognition by CAR-T cells requires antigen expression for robust antitumor efficacy, which results in escape and growth by tumor cells that do not express the target antigen.[39] To address this issue, an attractive strategy is to develop single CAR-T cells that can recognize multiple tumor antigens. CD19/CD20 or CD19/CD22 bispecific CAR-T cells have demonstrated robust clinical efficacy in patients with B cell malignancies.[40,41] We formed a tandem connection between FAP scFv and GPC3 scFv in one CAR molecule, leading to one CAR-T cell that could recognize FAP and GPC3 expressed on tumor cells. This design may address immune evasion caused by tumor antigen heterogeneity.

The immunosuppressive microenvironment is another challenge for CAR-T cell treatment of solid tumors. CAFs are the main cell type in the tumor stroma.[42] CAFs secrete many tumor growth factors, such as VEGFA, epidermal growth factor (EGF), and collagens, to remodel the tumor microenvironment and promote tumor growth and metastasis.[43–45] One attractive stromal cell target is FAP, and FAP remodels the tumor extracellular matrix and is a marker of CAFs.[22] FAP-targeting CAR-T cells could significantly eliminate CAFs and enhance the subsequent anti-PDAC efficacy of CAR-T cells targeting CLDN18.2 *in vivo*.[46] A study showed that FAP CAR-T cells decreased tumor growth without severe toxicity.[47] Therefore, GPC3 and FAP CAR-T cells can not only target tumor cells expressing FAP but also kill CAFs in tumors to increase efficacy *in vivo*.

Further studies will be needed to improve the persistence of CAR-T cells *in vivo*. As we showed in the HepG2 mouse model, the CAR-T cells had poor proliferation in the mouse model after being injected (Figures 4D and 5D). This may result from the fact that CAR-T cells differentiate from effector T cells to exhausted or dysfunctional T cells.[48] Controlling CAR signaling by controlling CAR affinity may promote the persistence of T cells.[49,50] Additionally, CAR signaling motifs and different cytokines are important. The 4-1BB, ICOS, and OX40 domains were shown to improve persistence in preclinical models.[51–54] Therefore, we can modify the design of CAR molecules by selecting the signaling domain, cytokine secretion, and affinity of scFv to enhance FAP-GPC3 bispecific CAR-T cell persistence and further improve antitumor efficacy *in vivo*.

Currently, there are several GPC3-targeting CAR-T cell therapies undergoing clinical trials,[55,56] yet there are no reports of significant side effects associated with GPC3 targeting. Concurrently, clinical trials for drugs targeting FAP are ongoing,[57] and no safety concerns have been reported. Nevertheless, studies in mice have indicated that

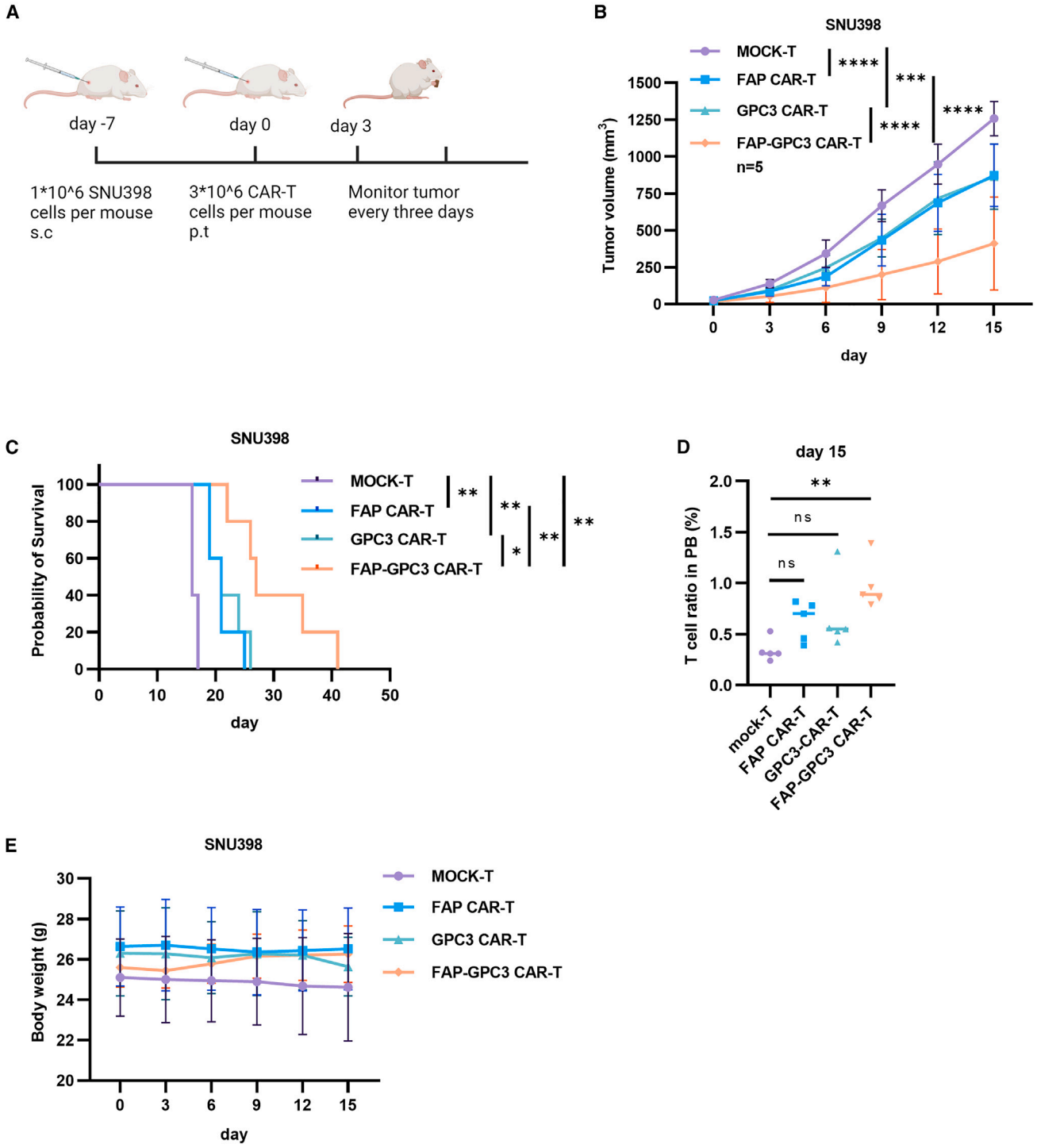

Figure 5. FAP-GPC3 CAR-T cells showed a potent suppressive effect on SNU398 CDX

(A) Schematic representation of the animal experiments with SNU398 CDX model. The graphical abstract was created with BioRender.com, agreement number: WL25RFHW4I. (B) Measurement of tumor volumes after treatment with CAR-T cells. The data are shown as the mean ± SD; two-way ANOVA with Tukey's multiple comparisons test; $^{*}p < 0.05$; $^{**}p < 0.01$; $^{***}p < 0.001$; $^{****}p \leq 0.0001$. (C) Kaplan-Meier survival curve showing overall survival; log rank (Mantel-Cox) test; $^{*}p < 0.05$; $^{**}p < 0.01$. (D) Human T cell ratios in the peripheral blood of SNU398 CDX model mice, detected by flow cytometry. The data are shown as the mean ± SD; two-way ANOVA with Tukey's multiple comparisons test; $^{**}p < 0.01$. (E) Mouse body weight in the SNU398 model.

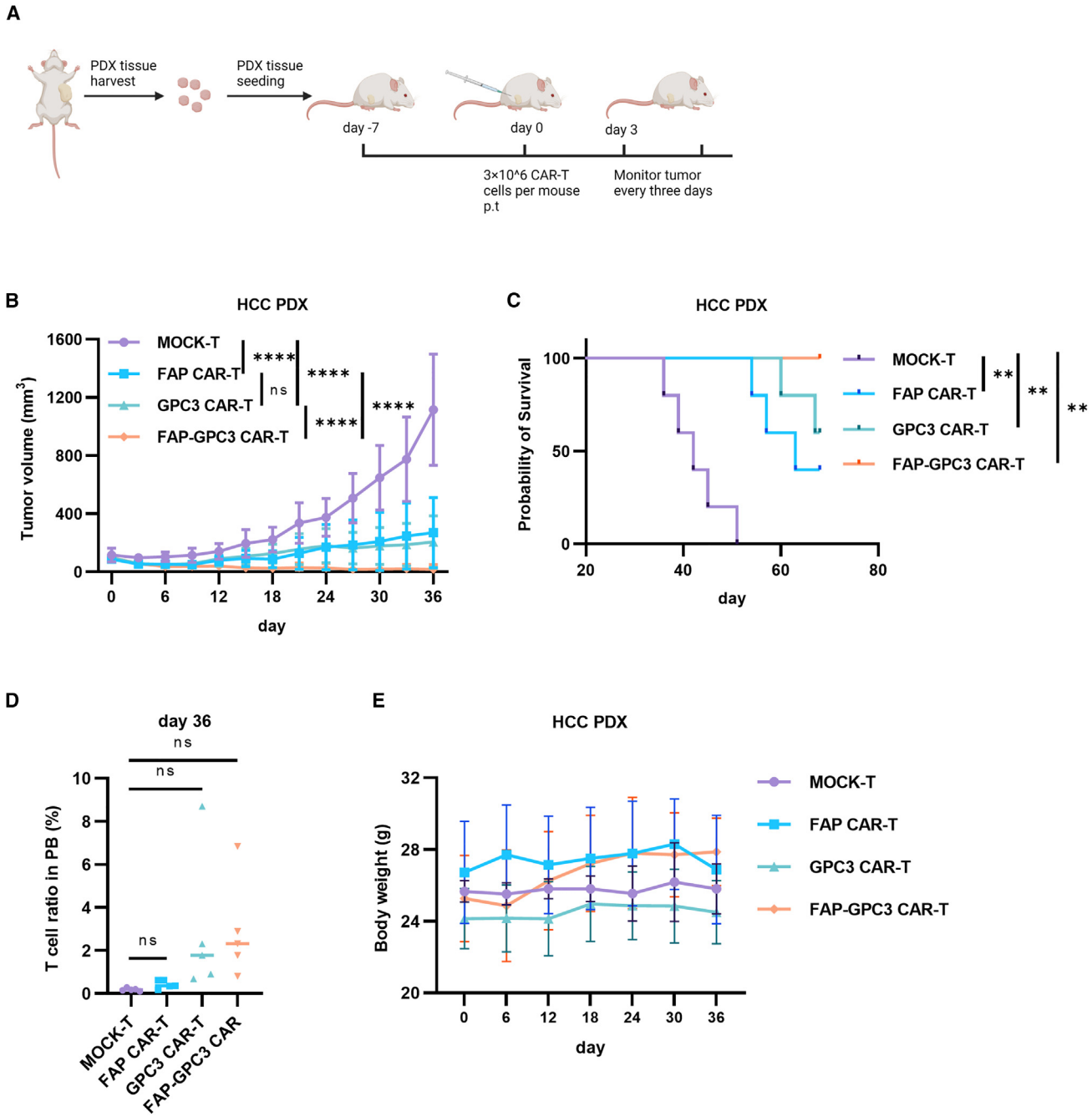

Figure 6. FAP-GPC3 CAR-T cells exhibited potent activity against HCC PDX

(A) Schematic representation of the animal experiments with PDX model. The graphical abstract was created with BioRender.com, agreement number: TN25RFGJSO. (B) Measurement of tumor volumes after treatment with CAR-T cells. The data are shown as the mean ± SD; two-way ANOVA with Tukey's multiple comparisons test; ****$p \leq 0.0001$. (C) Kaplan-Meier survival curve showing overall survival; log rank (Mantel-Cox) test; *$p < 0.05$; **$p < 0.01$. (D) Human T cell ratios in the peripheral blood of PDX model mice, detected by flow cytometry. The data are shown as the mean ± SD; two-way ANOVA with Tukey's multiple comparisons test. (E) Mouse body weight in the PDX model.

CAR-T cells targeting FAP do not induce obvious *in vivo* side effects.[47] The anti-FAP scFv utilized in this research could recognize both human and murine FAP.[58] Notably, in the three tumor-bearing mouse models investigated in this study, no significant changes in body weight or health issues were observed in the mice following the administration of bispecific CAR-T cells throughout the

treatment period. This finding suggests that bispecific CAR-T cells targeting FAP and GPC3 do not cause substantial side effects in mice. Since SNU387 failed to form tumors in immunodeficient mice, we have not yet performed *in vivo* experiments in tumor models expressing only FAP. Subsequently, we will use a tumor model overexpressing FAP to verify the safety of bispecific CAR-T cells in mice. Hence, theoretically, the bispecific CAR-T cell targeting FAP and GPC3 demonstrates a certain level of safety. However, further clinical trials are imperative to validate this claim. Consequently, additional safety studies pertaining to bispecific CAR-T cells will be conducted.

Here, we constructed bispecific CAR-T cells targeting GPC3 and FAP, and these bispecific CAR-T cells could recognize and kill tumor cells expressing FAP or GPC3. Bispecific CAR-T cells demonstrated more potent antitumor efficacy than any single-target CAR-T cells *in vitro* and *in vivo*. In conclusion, the strategy of two tandem scFvs in one CAR molecule is available, and bispecific GPC3 and FAP CAR-T cells may provide a new solution for HCC patient therapy and reduce tumor recurrence caused by antigen heterogeneity.

MATERIALS AND METHODS

GEO data analysis and patient survival analysis

The microarray data were downloaded from the GEO database: http://www.ncbi.nih.gov/geo. The raw data were downloaded as MINiML files. The files contain the data for all platforms, samples, and GSE records. The extracted data were normalized by log2 transformation. The microarray data were normalized by the normalize quantiles function of the preprocessCore package in R software (version 3.4.1). Probes were converted to gene symbols according to the annotation information of the normalized data in the platform. Probes matching multiple genes were removed from these datasets. The average expression value of the gene measured by multiple probes was calculated as the final expression value. To address the same dataset and platform but in different batches, the removeBatchEffect function of the limma package in R software was used to remove batch effects. To address different datasets or the same dataset but in different platforms, extract multiple datasets with common gene symbols and mark different datasets or different platforms as different batches, the removeBatchEffect function of the limma package in R software was used to remove batch effects. The result of the data preprocessing was assessed by a boxplot. The PCA plot was drawn to show the samples before and after the batch effect. All analyses were performed on Assistant of Clinical Bioinformatics (www.aclbi.com). Patient survival analysis was performed with Kaplan-Meier Plotter (KMplot.com).[59] The two patient cohorts were compared by a Kaplan-Meier survival plot, and the hazard ratio with 95% confidence intervals and log rank *p* value were calculated.

CAR vector constructs and lentivirus production

Third-generation anti-FAP, anti-GPC3, and anti-FAP-GPC3 CARs containing CD28 and TLR2 costimulatory molecules, CD3ζ signaling domains, and a tagged eGFP reporter gene were used. The anti-FAP scFv (FAP scFv sequence was reported in PCT/US10/02660) and anti-GPC3 scFv[60] in anti-FAP-GPC3 CARs were linked by a G4S linker. Lentiviral particles were produced in HEK-293T cells via polyethyleneimine (Sigma-Aldrich, St. Louis, MO, USA) transfection. A pWPXLd-based transfer plasmid and the packaging and envelope plasmids psPAX2 and pMD2.G were cotransfected into HEK-293T cells in 10-cm dishes. Supernatant containing the lentivirus was harvested at 24, 48, and 72 h after transfection and filtered through a 0.22-μm filter. A large amount of lentivirus was produced and stored in an ultra-low temperature refrigerator for subsequent experiments.

Generation of CAR-T cells

Peripheral blood mononuclear cells (PBMCs) were isolated from the PB of healthy adult donors using Lymphoprep (Stem Cell Technologies, Vancouver, Canada). T cells were negatively selected from PBMCs using a Human T cell Isolation Kit (Stem Cell Technologies, Vancouver, Canada). T cells were activated by TransAct (Miltenyi Biotec, Bergish Gladbach, Germany) for 36 h in GT-T551H3 medium (Takara Biotechnology Dalian, China) supplemented with 5% fetal bovine serum (FBS), 300 IU/mL IL-2, 10 mM HEPES, 2 mM glutamine, and 1% penicillin/streptomycin. After being activated, T cells were transduced with lentiviral supernatant in the presence of polybrene (Sigma-Aldrich, St. Louis, MO, USA) at a multiplicity of infection (MOI) of 5 for 12 h. Then, T cells were cultured in fresh GT-T551H3 medium containing FBS and IL-2 (300 U/mL), and fresh medium was added every 2 days to maintain the cell density at approximately 1×10^6 cells/mL. CAR expression was detected by flow cytometry with an anti-scFv cocktail (GeneScript, A02288, China). The healthy PBMC donors provided informed consent for the use of their samples for research purposes, and all procedures were approved by the Research Ethics Board of the Guangzhou Institutes of Biomedicine and Health, Chinese Academy of Sciences (GIBH).

Cells and culture conditions

HEK-293T cells, HepG2 cells, A549 cells, and AsPC-1 cells were maintained in Dulbecco's modified Eagle's medium (Gibco, Grand Island, NY, USA). SNU387 and SNU398 cells were maintained in RPMI-1640 medium (Gibco, Grand Island, NY, USA). The identities of the cell lines were confirmed by STR sequencing. The medium was supplemented with 10% heat-inactivated FBS (Gibco, Grand Island, NY, USA), 10 mM HEPES, 2 mM glutamine (Gibco, Grand Island, NY, USA), and 1% penicillin/streptomycin (Gibco, Grand Island, NY, USA). Luciferase/GFP-expressing cell lines (HepG2-GL, SNU387-GL, SNU398-GL, A549-GL, and AsPC-1-GL) were generated by transfecting the parental cell line with lentiviral supernatant containing luciferase-2A-GFP. FAP and GPC3 were respectively overexpressed in A549 and AsPC-1 cells by lentivirus transfection. All cells were cultured at 37°C in an atmosphere of 5% carbon dioxide.

In vitro tumor cell killing assays

The proportion of EGFP in each group of T cells was standardized by adding wild-type T cells, thus ensuring consistent proportions of CAR-T cells in each group. Then tumor target cells were incubated with MOCK-T cells, anti-FAP CAR-T cells, anti-GPC3 CAR-T cells, or anti-FAP-GPC3 CAR-T cells at the indicated ratios in triplicate in

white 96-well plates. Target cell viability was examined 24 h later by adding 100 μL/well D-luciferin (potassium salt) (Yeasen, China) at 150 μg/mL. Background luminescence was negligible (<1% of the signal from wells containing only target cells). Cytotoxicity was equal to (1 − (test RLU/no T cell average RLU)) ×100, where RLU is relative luminescent units.

Flow cytometry

The samples were analyzed using a NovoCyteTM (ACEA Biosciences), LSR Fortessa, or C6 flow cytometer (BD Biosciences), and the data were analyzed using FlowJo software (FlowJo, LLC, Ashland, OR, USA). The cells were stained with antibodies against human CD3-APC (clone UCHT1, BioLegend, San Diego, USA), CD25 (clone BC96, BioLegend, San Diego, USA), and CD69 (clone FN50, BioLegend, San Diego, USA) on ice for 30 min, and the cells were then washed with PBS containing 2% FBS before flow cytometric analysis. Cells expressing FAP and GPC3 were first stained with anti-FAP antibody (clone E1V9V, CST, USA) and rabbit-anti-GPC3 (D262896-0025, Sangon Biotech, China), washed with PBS a half an hour later, then stained with goat anti-rabbit immunoglobulin G conjugating Alex Fluor 647 (RS3811, ImmunoWay, China), and finally washed with PBS and resuspended. PB from xenografted mice was treated with red blood cell lysis buffer before being stained.

Cytokine release assays

ELISA kits for IL-2, IFN-γ, granzyme B, and TNF-α were purchased from DAKEWE (China). T cells were cocultured with target cells at an E:T ratio of 1:1 for 24 h. The culture supernatants were then collected and centrifuged at 300 relative centrifugal force for 5 min according to the protocols provided by the manufacturer.

Animal experiments

For tumor CDX models, 1×10^6 HepG2 cells or SNU398 cells were resuspended in 100 μL of PBS and injected subcutaneously into the right flank of NSI mice (6–8 weeks old). When the tumor nodes of most mice grew to approximately 30 mm^3, the mice were randomly divided into four groups (MOCK-T, FAP CAR-T, GPC3 CAR-T, and FAP-GPC3 CAR-T) and injected peritumorally with 3×10^6 CAR-T cells resuspended in 100 μL of PBS per mouse. Tumor volume and mouse body weight were measured twice per week (HepG2) or every 3 days (SNU398) with a caliper and calculated by the following equation: tumor volume = (length × $width^2$)/2. When the tumor volume reached 1,500 mm^3, the mice were euthanized by CO_2, and the time of euthanasia was recorded. When the tumor size of the first mouse reached 1,500 mm^3, orbital blood samples were collected from the mice to detect the proportion of T cells in the PB.

For PDX models, primary HCC tumors were placed in RPMI 1640 maintained in an ice bath. The tumors were then sliced into pieces of approximately 25 mm^3. Subsequently, the tissue was transplanted subcutaneously into the right flank of 8-week-old male NSI mice. The growth of the established tumor xenografts was routinely monitored at least twice a week. For serial transplantation, tumor-bearing animals were euthanized by diethyl ether anesthesia followed by cervical dislocation. The tumors were minced under sterile conditions and transplanted into successive NSI mice following the same procedure.

The animal experiments were performed in the Laboratory Animal Center of GIBH, Chinese Academy of Sciences. All animal procedures were approved by the Animal Welfare Committee of GIBH. All protocols were approved by the relevant Institutional Animal Care and Use Committee. All mice were maintained in specific pathogen-free (SPF)-grade cages and were provided autoclaved food and water.

Statistical analysis

Statistical significance was determined using Student's t test (two groups) or ANOVA with Tukey's multiple comparison test (three or more groups). All statistical analyses were performed using Prism software, version 7.0 (GraphPad, Inc., San Diego, CA, USA). Kaplan-Meier survival curves of *in vivo* data were analyzed using the log rank test. p values < 0.05 were considered statistically significant, and the following annotations were used: $^*p < 0.05$; $^{**}p < 0.01$; $^{***}p < 0.001$; and $^{****}p < 0.0001$.

DATA AND CODE AVAILABILITY

This study did not generate new unique data.

SUPPLEMENTAL INFORMATION

Supplemental information can be found online at https://doi.org/10.1016/j.omton.2024.200817.

ACKNOWLEDGMENTS

This study was supported by National Key Research and Development Plan, No. 2022YFE0210600; National Natural Science Foundation of China, No. 82341204 (P.L.), 82273377 (S.L.), 82202031 (L.Q.), 32370996 (L.Q.), and 32170946 (Z.J.); Science and Technology Planning Project of Guangdong Province, China (2023B1212060050, 2023B1212120009); The Youth Innovation Promotion Association of the Chinese Academy of Sciences, No. 2020351 (Z.J.), 2023371(S.L.); Guangdong Basic and Applied Basic Research Foundation, No. 2021A1515110005 (L.Q.), 2021A1515220077 (S.L.), 2022A1515012569 (Z.J.), 2022A1515012484 (S.L.), 2022A1515012360 (L.Q.), 2022A1515012569 (Z.J), 2022A1515010604 (Y.Y.), and 2022A1515110349 (D.Z.); 2020B1212060052; The University Grants Committee/Research Grants Council of the Hong Kong Special Administrative Region, China (Project No. AoE/M-401/20), Innovation and Technology Fund (ITF); Guangdong-Hong Kong-Macau Joint Laboratory of Respiratory Infectious Diseases (2019B121205010); Basic Research Project of Guangzhou Institutes of Biomedicine and Health, Chinese Academy of Sciences, No. GIBHBRP23-03 (P.L.); International Partnership Program of The Chinese Academy of Sciences No. 188GJHZ2022015GC (P.L.); Open Project of State Key Laboratory of Respiratory Disease, No. SKLRD-OP-202405 (Z.Z); and Science and Technology Projects in Guangzhou, China No. 2024B03J1232 (P.L.).

The graphical abstract was created with BioRender.com, agreement number: UX26H3EJR7.

AUTHOR CONTRIBUTIONS

P.Li, L.Z., and Y.L. conceived and designed the research. L.Z. and Y.L. performed the *in vitro* assays and animal experiments. P.Li, L.Z., and Y.L. wrote the manuscript. D.Z. provided important research reagents and technical advice. Y.Z. contributed to the animal experiments. D.Z., Y.C., and L.Q. provided critical advice on this study and revised the manuscript. D.P. performed T cell isolation. All authors revised and approved the manuscript.

DECLARATION OF INTERESTS

Peng Li is a scientific founder of GZI and GZCB and has equity in GZI and GZCB. Patent (application no. ZL202110257363.3) is authorized and Peng Li, L.Z., C.T., Z.J., Y.Y., and D.H. are inventors.

REFERENCES

1. Llovet, J.M., Zucman-Rossi, J., Pikarsky, E., Sangro, B., Schwartz, M., Sherman, M., and Gores, G. (2016). Hepatocellular carcinoma. Nat. Rev. Dis. Prim. *2*, 16018. https://doi.org/10.1038/nrdp.2016.18.
2. Forner, A., Reig, M., and Bruix, J. (2018). Hepatocellular carcinoma. Lancet *391*, 1301–1314. https://doi.org/10.1016/S0140-6736(18)30010-2.
3. Yang, J., Pan, G., Guan, L., Liu, Z., Wu, Y., Liu, Z., Lu, W., Li, S., Xu, H., and Ouyang, G. (2022). The burden of primary liver cancer caused by specific etiologies from 1990 to 2019 at the global, regional, and national levels. Cancer Med. *11*, 1357–1370. https://doi.org/10.1002/cam4.4530.
4. Testa, U., Pelosi, E., and Castelli, G. (2022). Clinical value of identifying genes that inhibit hepatocellular carcinomas. Expert Rev. Mol. Diagn. *22*, 1009–1035. https://doi.org/10.1080/14737159.2022.2154658.
5. Llovet, J.M., Montal, R., Sia, D., and Finn, R.S. (2018). Molecular therapies and precision medicine for hepatocellular carcinoma. Nat. Rev. Clin. Oncol. *15*, 599–616. https://doi.org/10.1038/s41571-018-0073-4.
6. Li, L., and Wang, H. (2016). Heterogeneity of liver cancer and personalized therapy. Cancer Lett. *379*, 191–197. https://doi.org/10.1016/j.canlet.2015.07.018.
7. Hay, K.A., and Turtle, C.J. (2017). Chimeric Antigen Receptor (CAR) T Cells: Lessons Learned from Targeting of CD19 in B-Cell Malignancies. Drugs *77*, 237–245. https://doi.org/10.1007/s40265-017-0690-8.
8. Boyiadzis, M.M., Dhodapkar, M.V., Brentjens, R.J., Kochenderfer, J.N., Neelapu, S.S., Maus, M.V., Porter, D.L., Maloney, D.G., Grupp, S.A., Mackall, C.L., et al. (2018). Chimeric antigen receptor (CAR) T therapies for the treatment of hematologic malignancies: clinical perspective and significance. J. Immunother. Cancer *6*, 137. https://doi.org/10.1186/s40425-018-0460-5.
9. Milone, M.C., Xu, J., Chen, S.J., Collins, M.A., Zhou, J., Powell, D.J., Jr., and Melenhorst, J.J. (2021). Engineering enhanced CAR T-cells for improved cancer therapy. Nat. Cancer *2*, 780–793. https://doi.org/10.1038/s43018-021-00241-5.
10. Yamauchi, N., Watanabe, A., Hishinuma, M., Ohashi, K.I., Midorikawa, Y., Morishita, Y., Niki, T., Shibahara, J., Mori, M., Makuuchi, M., et al. (2005). The glypican 3 oncofetal protein is a promising diagnostic marker for hepatocellular carcinoma. Mod. Pathol. *18*, 1591–1598. https://doi.org/10.1038/modpathol.3800436.
11. Iglesias, B.V., Centeno, G., Pascuccelli, H., Ward, F., Peters, M.G., Filmus, J., Puricelli, L., and de Kier Joffé, E.B. (2008). Expression pattern of glypican-3 (GPC3) during human embryonic and fetal development. Histol. Histopathol. *23*, 1333–1340. https://doi.org/10.14670/HH-23.1333.
12. Baumhoer, D., Tornillo, L., Stadlmann, S., Roncalli, M., Diamantis, E.K., and Terracciano, L.M. (2008). Glypican 3 expression in human nonneoplastic, preneoplastic, and neoplastic tissues: a tissue microarray analysis of 4,387 tissue samples. Am. J. Clin. Pathol. *129*, 899–906. https://doi.org/10.1309/HCQWPWD50XHD2DW6.
13. Capurro, M., Wanless, I.R., Sherman, M., Deboer, G., Shi, W., Miyoshi, E., and Filmus, J. (2003). Glypican-3: a novel serum and histochemical marker for hepatocellular carcinoma. Gastroenterology *125*, 89–97. https://doi.org/10.1016/s0016-5085(03)00689-9.
14. Li, N., Gao, W., Zhang, Y.F., and Ho, M. (2018). Glypicans as Cancer Therapeutic Targets. Trends Cancer *4*, 741–754. https://doi.org/10.1016/j.trecan.2018.09.004.
15. Pang, N., Shi, J., Qin, L., Chen, A., Tang, Y., Yang, H., Huang, Y., Wu, Q., Li, X., He, B., et al. (2021). IL-7 and CCL19-secreting CAR-T cell therapy for tumors with positive glypican-3 or mesothelin. J. Hematol. Oncol. *14*, 118. https://doi.org/10.1186/s13045-021-01128-9.
16. Fu, Y., Urban, D.J., Nani, R.R., Zhang, Y.F., Li, N., Fu, H., Shah, H., Gorka, A.P., Guha, R., Chen, L., et al. (2019). Glypican-3-Specific Antibody Drug Conjugates Targeting Hepatocellular Carcinoma. Hepatology *70*, 563–576. https://doi.org/10.1002/hep.30326.
17. Ishiguro, T., Sano, Y., Komatsu, S.I., Kamata-Sakurai, M., Kaneko, A., Kinoshita, Y., Shiraiwa, H., Azuma, Y., Tsunenari, T., Kayukawa, Y., et al. (2017). An anti-glypican 3/CD3 bispecific T cell-redirecting antibody for treatment of solid tumors. Sci. Transl. Med. *9*, eaal4291. https://doi.org/10.1126/scitranslmed.aal4291.
18. Jiang, Z., Jiang, X., Chen, S., Lai, Y., Wei, X., Li, B., Lin, S., Wang, S., Wu, Q., Liang, Q., et al. (2016). Anti-GPC3-CAR T Cells Suppress the Growth of Tumor Cells in Patient-Derived Xenografts of Hepatocellular Carcinoma. Front. Immunol. *7*, 690. https://doi.org/10.3389/fimmu.2016.00690.
19. Shi, D., Shi, Y., Kaseb, A.O., Qi, X., Zhang, Y., Chi, J., Lu, Q., Gao, H., Jiang, H., Wang, H., et al. (2020). Chimeric Antigen Receptor-Glypican-3 T-Cell Therapy for Advanced Hepatocellular Carcinoma: Results of Phase I Trials. Clin. Cancer Res. *26*, 3979–3989. https://doi.org/10.1158/1078-0432.CCR-19-3259.
20. Dal Bo, M., De Mattia, E., Baboci, L., Mezzalira, S., Cecchin, E., Assaraf, Y.G., and Toffoli, G. (2020). New insights into the pharmacological, immunological, and CAR-T-cell approaches in the treatment of hepatocellular carcinoma. Drug Resist. Updates *51*, 100702. https://doi.org/10.1016/j.drup.2020.100702.
21. Sun, L., Gao, F., Gao, Z., Ao, L., Li, N., Ma, S., Jia, M., Li, N., Lu, P., Sun, B., et al. (2021). Shed antigen-induced blocking effect on CAR-T cells targeting Glypican-3 in Hepatocellular Carcinoma. J. Immunother. Cancer *9*, e001875. https://doi.org/10.1136/jitc-2020-001875.
22. Fitzgerald, A.A., and Weiner, L.M. (2020). The role of fibroblast activation protein in health and malignancy. Cancer Metastasis Rev. *39*, 783–803. https://doi.org/10.1007/s10555-020-09909-3.
23. Claus, C., Ferrara, C., Xu, W., Sam, J., Lang, S., Uhlenbrock, F., Albrecht, R., Herter, S., Schlenker, R., Hüsser, T., et al. (2019). Tumor-targeted 4-1BB agonists for combination with T cell bispecific antibodies as off-the-shelf therapy. Sci. Transl. Med. *11*, eaav5989. https://doi.org/10.1126/scitranslmed.aav5989.
24. Rurik, J.G., Tombácz, I., Yadegari, A., Méndez Fernández, P.O., Shewale, S.V., Li, L., Kimura, T., Soliman, O.Y., Papp, T.E., Tam, Y.K., et al. (2022). CAR T cells produced in vivo to treat cardiac injury. Science *375*, 91–96. https://doi.org/10.1126/science.abm0594.
25. Yang, X., Lin, Y., Shi, Y., Li, B., Liu, W., Yin, W., Dang, Y., Chu, Y., Fan, J., and He, R. (2016). FAP Promotes Immunosuppression by Cancer-Associated Fibroblasts in the Tumor Microenvironment via STAT3-CCL2 Signaling. Cancer Res. *76*, 4124–4135. https://doi.org/10.1158/0008-5472.CAN-15-2973.
26. Garin-Chesa, P., Old, L.J., and Rettig, W.J. (1990). Cell surface glycoprotein of reactive stromal fibroblasts as a potential antibody target in human epithelial cancers. Proc. Natl. Acad. Sci. USA *87*, 7235–7239. https://doi.org/10.1073/pnas.87.18.7235.
27. Kraman, M., Bambrough, P.J., Arnold, J.N., Roberts, E.W., Magiera, L., Jones, J.O., Gopinathan, A., Tuveson, D.A., and Fearon, D.T. (2010). Suppression of antitumor immunity by stromal cells expressing fibroblast activation protein-alpha. Science *330*, 827–830. https://doi.org/10.1126/science.1195300.
28. McAndrews, K.M., Chen, Y., Darpolor, J.K., Zheng, X., Yang, S., Carstens, J.L., Li, B., Wang, H., Miyake, T., Correa de Sampaio, P., et al. (2022). Identification of Functional Heterogeneity of Carcinoma-Associated Fibroblasts with Distinct IL6-Mediated Therapy Resistance in Pancreatic Cancer. Cancer Discov. *12*, 1580–1597. https://doi.org/10.1158/2159-8290.CD-20-1484.
29. Zou, B., Liu, X., Zhang, B., Gong, Y., Cai, C., Li, P., Chen, J., Xing, S., Chen, J., Peng, S., et al. (2018). The Expression of FAP in Hepatocellular Carcinoma Cells is Induced by

Hypoxia and Correlates with Poor Clinical Outcomes. J. Cancer *9*, 3278–3286. https://doi.org/10.7150/jca.25775.

30. Jiang, Z., Cheng, L., Wu, Z., Zhou, L., Wang, H., Hong, Q., Wu, Q., Long, Y., Huang, Y., Xu, G., et al. (2022). Transforming primary human hepatocytes into hepatocellular carcinoma with genetically defined factors. EMBO Rep. *23*, e54275. https://doi.org/10.15252/embr.202154275.

31. June, C.H., O'Connor, R.S., Kawalekar, O.U., Ghassemi, S., and Milone, M.C. (2018). CAR T cell immunotherapy for human cancer. Science *359*, 1361–1365. https://doi.org/10.1126/science.aar6711.

32. Lai, Y., Weng, J., Wei, X., Qin, L., Lai, P., Zhao, R., Jiang, Z., Li, B., Lin, S., Wang, S., et al. (2018). Toll-like receptor 2 costimulation potentiates the antitumor efficacy of CAR T Cells. Leukemia *32*, 801–808. https://doi.org/10.1038/leu.2017.249.

33. Sendler, M., van den Brandt, C., Glaubitz, J., Wilden, A., Golchert, J., Weiss, F.U., Homuth, G., De Freitas Chama, L.L., Mishra, N., Mahajan, U.M., et al. (2020). NLRP3 Inflammasome Regulates Development of Systemic Inflammatory Response and Compensatory Anti-Inflammatory Response Syndromes in Mice With Acute Pancreatitis. Gastroenterology *158*, 253–269.e14. https://doi.org/10.1053/j.gastro.2019.09.040.

34. Corso, S., Isella, C., Bellomo, S.E., Apicella, M., Durando, S., Migliore, C., Ughetto, S., D'Errico, L., Menegon, S., Moya-Rull, D., et al. (2019). A Comprehensive PDX Gastric Cancer Collection Captures Cancer Cell-Intrinsic Transcriptional MSI Traits. Cancer Res. *79*, 5884–5896. https://doi.org/10.1158/0008-5472.CAN-19-1166.

35. Ye, W., Jiang, Z., Li, G.X., Xiao, Y., Lin, S., Lai, Y., Wang, S., Li, B., Jia, B., Li, Y., et al. (2015). Quantitative evaluation of the immunodeficiency of a mouse strain by tumor engraftments. J. Hematol. Oncol. *8*, 59. https://doi.org/10.1186/s13045-015-0156-y.

36. Chan, L.K., Tsui, Y.M., Ho, D.W.H., and Ng, I.O.L. (2022). Cellular heterogeneity and plasticity in liver cancer. Semin. Cancer Biol. *82*, 134–149. https://doi.org/10.1016/j.semcancer.2021.02.015.

37. Guedan, S., Ruella, M., and June, C.H. (2019). Emerging Cellular Therapies for Cancer. Annu. Rev. Immunol. *37*, 145–171. https://doi.org/10.1146/annurev-immunol-042718-041407.

38. Zhang, Q., Lou, Y., Yang, J., Wang, J., Feng, J., Zhao, Y., Wang, L., Huang, X., Fu, Q., Ye, M., et al. (2019). Integrated multiomic analysis reveals comprehensive tumour heterogeneity and novel immunophenotypic classification in hepatocellular carcinomas. Gut *68*, 2019–2031. https://doi.org/10.1136/gutjnl-2019-318912.

39. Boumahdi, S., and de Sauvage, F.J. (2020). The great escape: tumour cell plasticity in resistance to targeted therapy. Nat. Rev. Drug Discov. *19*, 39–56. https://doi.org/10.1038/s41573-019-0044-1.

40. Spiegel, J.Y., Patel, S., Muffly, L., Hossain, N.M., Oak, J., Baird, J.H., Frank, M.J., Shiraz, P., Sahaf, B., Craig, J., et al. (2021). CAR T cells with dual targeting of CD19 and CD22 in adult patients with recurrent or refractory B cell malignancies: a phase 1 trial. Nat. Med. *27*, 1419–1431. https://doi.org/10.1038/s41591-021-01436-0.

41. Cordoba, S., Onuoha, S., Thomas, S., Pignataro, D.S., Hough, R., Ghorashian, S., Vora, A., Bonney, D., Veys, P., Rao, K., et al. (2021). CAR T cells with dual targeting of CD19 and CD22 in pediatric and young adult patients with relapsed or refractory B cell acute lymphoblastic leukemia: a phase 1 trial. Nat. Med. *27*, 1797–1805. https://doi.org/10.1038/s41591-021-01497-1.

42. Fiori, M.E., Di Franco, S., Villanova, L., Bianca, P., Stassi, G., and De Maria, R. (2019). Cancer-associated fibroblasts as abettors of tumor progression at the crossroads of EMT and therapy resistance. Mol. Cancer *18*, 70. https://doi.org/10.1186/s12943-019-0994-2.

43. Fukumura, D., Xavier, R., Sugiura, T., Chen, Y., Park, E.C., Lu, N., Selig, M., Nielsen, G., Taksir, T., Jain, R.K., and Seed, B. (1998). Tumor induction of VEGF promoter activity in stromal cells. Cell *94*, 715–725. https://doi.org/10.1016/s0092-8674(00)81731-6.

44. De Palma, M., Biziato, D., and Petrova, T.V. (2017). Microenvironmental regulation of tumour angiogenesis. Nat. Rev. Cancer *17*, 457–474. https://doi.org/10.1038/nrc.2017.51.

45. Xing, F., Saidou, J., and Watabe, K. (2010). Cancer associated fibroblasts (CAFs) in tumor microenvironment. Front. Biosci. *15*, 166–179. https://doi.org/10.2741/3613.

46. Liu, Y., Sun, Y., Wang, P., Li, S., Dong, Y., Zhou, M., Shi, B., Jiang, H., Sun, R., and Li, Z. (2023). FAP-targeted CAR-T suppresses MDSCs recruitment to improve the antitumor efficacy of claudin18.2-targeted CAR-T against pancreatic cancer. J. Transl. Med. *21*, 255. https://doi.org/10.1186/s12967-023-04080-z.

47. Wang, L.C.S., Lo, A., Scholler, J., Sun, J., Majumdar, R.S., Kapoor, V., Antzis, M., Cotner, C.E., Johnson, L.A., Durham, A.C., et al. (2014). Targeting fibroblast activation protein in tumor stroma with chimeric antigen receptor T cells can inhibit tumor growth and augment host immunity without severe toxicity. Cancer Immunol. Res. *2*, 154–166. https://doi.org/10.1158/2326-6066.CIR-13-0027.

48. Wherry, E.J. (2011). T cell exhaustion. Nat. Immunol. *12*, 492–499. https://doi.org/10.1038/ni.2035.

49. Ghorashian, S., Kramer, A.M., Onuoha, S., Wright, G., Bartram, J., Richardson, R., Albon, S.J., Casanovas-Company, J., Castro, F., Popova, B., et al. (2019). Enhanced CAR T cell expansion and prolonged persistence in pediatric patients with ALL treated with a low-affinity CD19 CAR. Nat. Med. *25*, 1408–1414. https://doi.org/10.1038/s41591-019-0549-5.

50. Caruso, H.G., Hurton, L.V., Najjar, A., Rushworth, D., Ang, S., Olivares, S., Mi, T., Switzer, K., Singh, H., Huls, H., et al. (2015). Tuning Sensitivity of CAR to EGFR Density Limits Recognition of Normal Tissue While Maintaining Potent Antitumor Activity. Cancer Res. *75*, 3505–3518. https://doi.org/10.1158/0008-5472.CAN-15-0139.

51. Song, D.G., Ye, Q., Carpenito, C., Poussin, M., Wang, L.P., Ji, C., Figini, M., June, C.H., Coukos, G., and Powell, D.J., Jr. (2011). In vivo persistence, tumor localization, and antitumor activity of CAR-engineered T cells is enhanced by costimulatory signaling through CD137 (4-1BB). Cancer Res. *71*, 4617–4627. https://doi.org/10.1158/0008-5472.CAN-11-0422.

52. Guedan, S., Posey, A.D., Jr., Shaw, C., Wing, A., Da, T., Patel, P.R., McGettigan, S.E., Casado-Medrano, V., Kawalekar, O.U., Uribe-Herranz, M., et al. (2018). Enhancing CAR T cell persistence through ICOS and 4-1BB costimulation. JCI Insight *3*, e96976. https://doi.org/10.1172/jci.insight.96976.

53. Kawalekar, O.U., O'Connor, R.S., Fraietta, J.A., Guo, L., McGettigan, S.E., Posey, A.D., Jr., Patel, P.R., Guedan, S., Scholler, J., Keith, B., et al. (2016). Distinct Signaling of Coreceptors Regulates Specific Metabolism Pathways and Impacts Memory Development in CAR T Cells. Immunity *44*, 380–390. https://doi.org/10.1016/j.immuni.2016.01.021.

54. Zhao, Z., Condomines, M., van der Stegen, S.J.C., Perna, F., Kloss, C.C., Gunset, G., Plotkin, J., and Sadelain, M. (2015). Structural Design of Engineered Costimulation Determines Tumor Rejection Kinetics and Persistence of CAR T Cells. Cancer Cell *28*, 415–428. https://doi.org/10.1016/j.ccell.2015.09.004.

55. Chen, Y., E, C.Y., Gong, Z.W., Liu, S., Wang, Z.X., Yang, Y.S., and Zhang, X.W. (2018). Chimeric antigen receptor-engineered T-cell therapy for liver cancer. Hepatobiliary Pancreat. Dis. Int. *17*, 301–309. https://doi.org/10.1016/j.hbpd.2018.05.005.

56. Nishida, T., and Kataoka, H. (2019). Glypican 3-Targeted Therapy in Hepatocellular Carcinoma. Cancers *11*, 1339. https://doi.org/10.3390/cancers11091339.

57. Shahvali, S., Rahiman, N., Jaafari, M.R., and Arabi, L. (2023). Targeting fibroblast activation protein (FAP): advances in CAR-T cell, antibody, and vaccine in cancer immunotherapy. Drug Deliv. Transl. Res. *13*, 2041–2056. https://doi.org/10.1007/s13346-023-01308-9.

58. Fischer, E., Chaitanya, K., Wüest, T., Wadle, A., Scott, A.M., van den Broek, M., Schibli, R., Bauer, S., and Renner, C. (2012). Radioimmunotherapy of fibroblast activation protein positive tumors by rapidly internalizing antibodies. Clin. Cancer Res. *18*, 6208–6218. https://doi.org/10.1158/1078-0432.CCR-12-0644.

59. Menyhart, O., Nagy, A., and Gyorffy, B. (2018). Determining consistent prognostic biomarkers of overall survival and vascular invasion in hepatocellular carcinoma. R. Soc. Open Sci. *5*, 181006. https://doi.org/10.1098/rsos.181006.

60. Jiang, Z., Jiang, X., Chen, S., Lai, Y., Wei, X., Li, B., Lin, S., Wang, S., Wu, Q., Liang, Q., et al. (2016). Anti-GPC3-CAR T Cells Suppress the Growth of Tumor Cells in Patient-Derived Xenografts of Hepatocellular Carcinoma. Front. Immunol. *7*, 690. https://doi.org/10.3389/fimmu.2016.00690.